Self-Assembly of Multiwall Carbon Nanotubes from Quench-Condensed CNi_3 Films

D.P. Young, A.B. Karki, and P. W. Adams
Department of Physics and Astronomy
Louisiana State University
Baton Rouge, Louisiana, 70803

Johnpeter N. Ngunjiri and Jayne C. Garno
Department of Chemistry and the Center for Biomodular Multi-scale Systems
Louisiana State University
Baton Rouge, LA, 70803

Hongwei Zhu and Bingqing Wei*
Department of Electrical and Computer Engineering
Louisiana State University
Baton Rouge, LA 70803

D. Moldovan
Department of Mechanical Engineering
Louisiana State University
Baton Rouge, LA 70803
(Dated: October 8, 2007)

Freestanding, vertical, multiwall carbon nanotubes (MWCNT) are formed during the vacuum deposition of thin films of the metastable carbides CT_3 (T = Ni, Co) onto fire-polished glass substrates. In contrast to widely used chemical and laser vapor deposition techniques, we utilize direct e-beam evaporation of arc-melted CT_3 targets to produce MWCNs that are self-assembled out of the CT_3-film matrix. The depositions are made in an ambient vapor pressure that is at least six orders of magnitude lower than the $1-100$ Torr typically used in chemical vapor techniques. Furthermore the substrates need not be heated, and, in fact, we observe robust nanotube growth on liquid nitrogen cooled glass and sapphire substrates. High-resolution atomic force microscopy reveals that MWCNTs of heights $1-40$ nm are formed in films with nominal thicknesses in the range of $5-60$ nm. We show that the growth parameters of the nanotubes are very sensitive to the grain structure of the films. This is consistent with a precipitation mediated root-growth mechanism.

Almost immediately after their discovery in the early 1990's [1], it was recognized that carbon nanotubes exhibit extraordinary mechanical [2] and electrical [3] properties, and that these could be the basis of new technologies [4]. Clearly, however, one of the most important issues facing the development of nanotube-based applications in areas such as microelectronics, high strength materials, and high resolution displays, is the control and optimization of their growth processes. In many applications the growth of well characterized, aligned nanotubes on specific substrates is needed [4, 5]. Though successful, large-scale growth of aligned nanotubes has, in fact ,been achieved via plasma-enhanced chemical vapor deposition (CVD) on Si substrates patterned with Ni nanodots [6], CVD is carried out in a harsh high temperature environment in which the substrate must be heated above 500 ^{o}C. Consequently, this technique cannot be used to grow aligned carbon nanotubes on fragile substrates such as polymers and organics. We demonstrate that freestanding, vertical, multi-wall carbon nanotubes (MWCNT) can spontaneously self-assemble out of metastable carbide films formed by direct high vacuum e-beam deposition from CT_3 (T = Ni, Co) targets. We believe that the nanotube growth is driven by the precipitation of carbon out of hot CT_3 nanoparticles as they quench-condense onto the substrate. This process is extremely sensitive to the details of the nanoparticle geometry. Thus one should be able to achieve good control over the nanotube growth parameters by modulating the grain structure of the films.

Thin films of the metastable intermetallic CNi_3 [7, 8] were deposited onto liquid nitrogen (LN_2) cooled fire-polished glass and crystalline sapphire substrates by electron-beam evaporation of CNi_3 targets. The targets consisted of arcmelted buttons of high purity graphite (Johnson Matthey, 99.9999%) and nickel (Johnson Matthey, 99.999%). The buttons were made with a starting stoichiometry of $CNi_{3.25}$ to compensate for some loss of nickel during the melting process. The CNi_3 structure of the films was verified by x-ray diffraction [9]. The depositions were made onto fire-polished silica glass and polycrystalline Al_2O_3 substrates that were cooled to 84 K. Typical deposition rates were ~ 0.1 nm/s in a 2 μTorr vacuum. The film thickness was determined using a quartz-crystal monitor.

The CNi_3 targets exhibited excellent e-beam deposition characteristics. We did not observe spitting, and the

deposition rates were stable in the range of $0.1-1$ nm/s. The resulting films were metallic in appearance and adhered extremely well to the glass and sapphire substrates. We monitored the film resistance during deposition and found an unusually low threshold of electrical continuity on glass. In Fig. 1 we compare the thickness dependence of the dimensionless sheet conductance G of a Be film on glass with that of CNi_3 films on glass and sapphire. Beryllium is known to produce extremely smooth, dense, and homogeneously disordered films on LN_2-cooled glass [10], and this is evidenced by its remarkably low thickness-threshold of electrical continuity, ~ 1.0 nm. Note that the CNi_3 continuity threshold on glass, ~ 1.7 nm is comparable to that of the Be film but that CNi_3 films on sapphire have roughly a factor of two higher thickness threshold. A higher continuity threshold is generally indicative of larger grain sizes. (For instance, Pb, which has poor adhesion to most substrates, produces highly granular films whose continuity threshold is about 8 nm on LN_2-cooled glass.) Upon warming the films to room temperature and breaking the vacuum, we observed very little increase in the resistance of the CNi_3 films, indicative of the fact that they were quite stable in air.

Based upon the low continuity threshold and excellent conductance of films on glass substrates, we expected that atomic force microscopy (AFM) would reveal a homogeneously disordered, dense film base. An Agilent 5500 SPM equipped with PicoScan v5.3.3 software was used for AFM characterizations. Images were acquired using contact mode AFM in ambient conditions with oxide-sharpened silicon nitride cantilevers from Veeco Probes. Typical imaging forces were 1- 2 nN. The data was analyzed using Gwyddion v. 2.7 open source software. Shown in Fig. 2 are AFM micrographs of 5 nm thick film and a 60 nm thick CNi_3 film. Though the 5 nm film does, indeed, have an extraordinarily smooth base, an apparently random array of rectilinear spike-like structures are formed during the deposition process. Interestingly, the spikes extend as high as 40 nm out of what is nominally a very thin film. In contrast, the base of the 60 nm film is substantially rougher, with somewhat shorter and more numerous spikes extending upward. Shown in Fig. 3 is a transmission electron microscopy (TEM; JOEL 2010F) image of a sample prepared by immersing a CNi_3-coated glass substrate into ethanol and then sonicating it for 5 minutes. A drop of the resulting suspension was placed onto a C-coated copper grid, which was subsequently allowed to dry in air. The spikes are obviously multi-walled and have a hollow core, suggesting that they are carbon nanotubes. The electron diffraction pattern shown in the inset is consistent with the structure of MWCNT's. The interplanar lattice fringes are measured with spacings of $\sim$0.34 nm, in good agreement with the (002) planes of the rolled-up graphite layers in a MWCNT [3].

We believe that the nanotubes are growing directly out of the nickel carbide film. The fact that we only observed nanotubes oriented along the surface normal rules out the possibility that they are being deposited from the e-beam hearth. If, in fact, they were formed in the hearth and subsequently deposited onto the substrate, then we would expect to see a random arrangement of them in the AFM images [11], with very few, if any, standing straight up. We propose that the MWCNT are the product of self-assembled growth that is driven by the unusually strong temperature dependence of the solubility of C in Ni [12, 13]. The binary phase diagram of C-Ni does not contain any stable compounds and only one metastable compound CNi_3 [14]. At the melting point of CNi_3, $\sim 2500^oC$, there is 25 atomic percent carbon in solution. Below $\sim 1300^oC$, however, the saturated carbon concentration falls to less than 3% [15]. An interesting consequence of this solubility behavior is that arc-melted CNi_3 and CCo_3 buttons precipitate out a layer of graphite on the button surface as they cool to room temperature. The graphite crystallites, which are easily seen with the naked eye, have been verified via scanning electron microprobe elemental analysis. We believe that much of this carbon crust is reabsorbed into the button as it is brought up to deposition temperatures in the e-beam hearth. Recently we have shown that by exposing the CNi_3 films to hot magnesium vapor we can produce films of the non-conventional superconductor $MgCNi_3$ [9]. This suggests, of course, that the e-beam deposition proceeds at approximately the correct CNi_3 stoichiometry, and that, at room temperature, the films are supersaturated with carbon. Thus the carbon nanotubes form in response to the precipitation of graphite as hot CNi_3 vapor quench-condenses onto the cold substrate surface [12, 16].

The dissolution of carbon from transition metal nanoparticles can produce either a graphitic shell or, under the right conditions, nanotube structures [13, 16]. The competition between these two limiting growth modes depends critically on the details of the geometrical and chemical characteristics of the nanoparticle. A graphitic shell is thought to be the equilibrium structure in which the carbon wets the particle surface. It is possible, however, for the graphitic growth to become kinetically unstable in such a way as to produce carbon nantotubes. In this latter scenario the carbon no longer wets the entire surface of the metal particle, and the nanotube grows from the base up. There is an emerging consensus that catalyst particles of diameters 5 - 20 nm are needed for efficient nanotube nucleation [15, 17]. This would imply that the nanotube nucleation probability is sensitive to the details of the grain structure of the films. TEM analysis of 10 nm thick CNi_3 films on glass indicates an average matrix grain size of $R \sim 6$ nm. If one assumes that the diffusivity of C in Ni is comparable to that of C in fcc Fe at 1100 ^{o}C, $D \sim 5\text{x}10^{-11}$ m^2/s [18], then C will precipitate out of a 10 nm diameter Ni grain in $t_{diff} = R^2/D \sim 1\mu$s. At a deposition rate of ~ 0.2 nm/s, it takes about 1 min to form a 10 nm film. Therefore the nanotubes are self-assembling almost instantly on

deposition timescales.

In Fig. 4 we present the results of a statistical analysis of numerous AFM micrographs of CNi_3 films of varying thickness d. We have also observed robust nanotube growth in CCo_3 films on glass. However, at present we do not have a sufficiently broad range of CCo_3 films to warrant a statistical study, hence we will restrict our discussion to the CNi_3 system. All of the films used in this analysis were deposited onto glass under identical conditions. In Fig. 4 we plot the areal nanotube density as a function of film thickness. Note that the density initially grows with increasing film thickness but saturates in films with $d > 35$ nm. The data also suggest that very few, if any, nanotubes are formed in films thinner than ~ 5 nm. We have developed a simple model to explain these thickness dependences. The model invokes several simplifying assumptions. The first is that the grain structure of the film is independent of d, and, therefore, the nucleation probability is also independent of d. The second assumption is that, because the nanotubes assemble almost instantly, the film can be broken into n discreet sublayers, each having a minimal thickness Δd necessary for the production of an areal nanotube density N_o. Within the context of the model, the net nanotube density is built up by stacking n such layers as shown in the inset of Fig. 4, with the constraint that $d = n\Delta d$. As the layers are stacked a portion of the lower nanotube population gets *buried* by the upper layers. It is only those nanotubes that extend through the uppermost layer that are imaged by AFM. Therefore the population statistics are completely governed by the convolution of this burying effect with the intrinsic nanotube height distribution of a single sublayer.

The salient features of the model can be obtained with a uniform carbon nanotube height distribution $\rho(h) = N_o/h_m$ in the interval $[0, h_m]$, where h_m is the maximum nanotube height (Fig. 4 inset). Of course, h_m is determined by the details of the film morphology and nucleation properties, which are beyond the scope of the model. Notwithstanding this limitation, it is relatively easy to show that the model predicts that the nanotube number density is quadratic in d,

$$N(d) = \frac{N_o h_m}{\Delta d}\left[\frac{d-d_o}{h_m} - \frac{(d-d_o)^2}{2h_m^2}\right], \tag{1}$$

up to a critical thickness $d_{cr} = d_o + h_m$. Beyond this point the density remains constant at $N(d_{cr})$. The parameter d_o represents the minimum thickness for the nucleation of nanotube growth. It is reasonable to assume that Δd is constrained by this parameter, $\Delta d \sim d_o$. The dashed line in Fig. 4 reflects a fit of Eq. (1) to the data in which $N_o = 3$ μm^{-2} and $h_m = 32$ nm were varied. We took $d_0 = \Delta d = 3$ nm. The model give an excellent fit to the data in Fig. 4. As a consistency check, we note that the nanotube density of the 5 nm film in Fig. 2 is ~ 1 μm^{-2}. This is reasonably close to the value of N_o extracted from the fit. Furthermore, the height of the tallest nanotubes in Fig. 2 is comparable to the value of h_m obtained from the fit.

Though the model correctly predicts the general features of $N(d)$, it does not address the microscopic details that govern the nucleation and structure of the multi-wall nanotubes. We believe that these aspects of the growth are largely dependent upon the micromorphology of the film, which is, in turn, sensitive to a number of parameters including deposition rate, deposition temperature, and substrate chemistry. Indeed, this sensitivity is evident in the micrographs of Fig. 5, where we compare nanotube growth in CNi_3 on glass with that of films on sapphire. As discussed earlier we believe that films on sapphire are significantly more granular than those on glass (see Fig. 1). In accord, a cursory comparison of the two images in Fig. 5 shows a much higher nanotube density on sapphire, clearly indicating nanotube nucleation is much more favorable on this substrate.

In summary, we have demonstrated that multiwall carbon nanotubes can self-assemble from CNi_3 and CCo_3 films deposited onto liquid nitrogen cooled substrates. In contrast to CVD techniques, this low temperature process is compatible with standard silicon photoresist patterning technologies and may provide a viable strategy for producing aligned multiwall nanotubes on fragile substrates such as organics and polymers. Furthermore, direct root growth out of metastable carbide films allows one to produce very high density arrays of aligned posts, which could prove useful in molecular sieve applications [19, 20]. It should be possible to control the MWCNT growth parameters by manipulating the film microstructure via the deposition parameters, substrate modifiers, and/or annealing protocols.

We gratefully acknowledge enlightening discussions with Ilya Vekhter and Dana Browne. PWA acknowledges the support of the DOE under Grant No. DE-FG02-07ER46420. DPY acknowledges support of the NSF under Grant No. DMR-0449022.

---

* Present address: Department of Mechanical Engineering, University of Delaware, Newark, DE 19716

[1] S. Iijima, Nature **354**, 56 (1991).

[2] D. H. Robertson, D. W. Brenner, and J. W. Mintmire, Phys. Rev. B **45**, 12592 (1992).
[3] R. Saito, M. Fujita, G. Dresselhaus, and M. S. Dresselhaus, Phys. Rev. B **46**, 1804 (1992).
[4] P. G. Colllins and A. Zettl, Phys. Rev. B **55**, 9391 (1997).
[5] J. Wen, Z. Huang, D. Wang, J. Chen, S. Yang, Z. Ren, J. Wang, L. Calvet, J. Chen, J. Klemic, et al., J. Mater. Res. **16**, 3246 (2001).
[6] Z. F. Ren, Z. P. Huang, J. W. Xu, J. H. Wang, P. Bush, M. P. Siegal, and P. N. Provencio, Science **282**, 1105 (1998).
[7] R. Yue, R. Sabiryanov, E. Kirkpatrick, and D. Leslie-Pelecky, Phys. Rev. B **62**, 8969 (2000).
[8] D. Lelslie-Pelecky, X. Zhang, S. Kim, M. Bonder, and R. Rieke, Chem. Mat. **10**, 164 (1998).
[9] D. Young, M. Moldovan, D. Craig, P. Adams, and J. Chan, Phys. Rev. B **68**, 020501 (2003).
[10] V. Y. Butko, J. F. DiTusa, and P. W. Adams, Phys. Rev. Lett. **84**, 1543 (2000).
[11] K. Yamamoto, Y. Koga, S. Fujiwara, and K. Masaaki, Appl. Phys. Lett. **69**, 4174 (1996).
[12] A. Maiti, C. Brabec, and J. Bernhole, Phys. Rev. B **55**, R6097 (1997).
[13] A. Loiseau, J. Gavillet, F. Ducastelle, J. Thibault, O. Stephan, P. Bernier, and S. Thair, C.R. Physique **4**, 975 (2003).
[14] K. Natesan and T. Kassner, Metall. Trans. **4**, 2557 (1973).
[15] H. Kanzow and A. Ding, Phys. Rev. B **60**, 11180 (1999).
[16] J. Gavillet, A. Loiseau, C. Journet, F. Willaime, F. Ducastelle, and J. Charlier, Phys. Rev. Lett. **87**, 275504 (2001).
[17] S. Helveg, C. López-Cartes, J. Sehested, P. Hansen, B. Clausen, J. Rostrup-Nielsen, F. Ablid-Pedersen, and J. Nørskov, Nature **427**, 426 (2004).
[18] E. Brandes and G. Brooks, eds., *Smithells Metals Reference Book* (Butterworth-Heinemann, Oxford, 1992), 7th ed.
[19] W. Volkmuth and R. Austin, Nature **358**, 600 (1992).
[20] N. Kaji, Y. Tezuka, Y. Takamura, M. Ueda, T. Nishimoto, H. Nakanishi, Y. Horlike, and Y. Baba, Anal. Chem. **76**, 15 (2004).

Figures

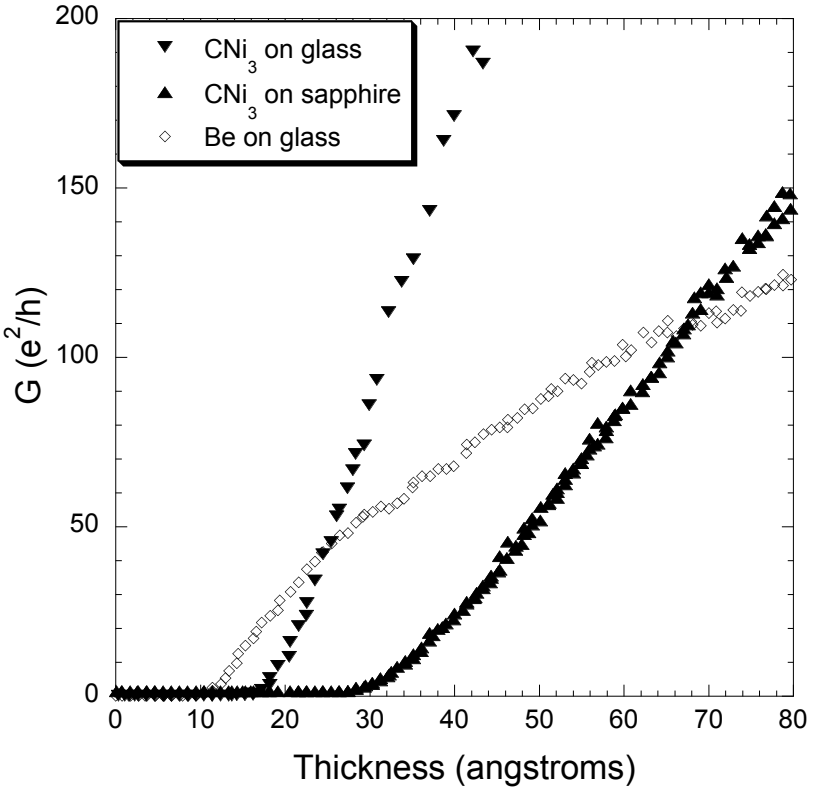

FIG. 1: Comparison of the thickness dependence of the dimensionless sheet conductance of a beryllium deposited on a glass substrate along with that of a CNi_3 film on glass and one on sapphire. All of the films were deposited onto liquid nitrogen cooled substrates held at 84 K. The conductance measurements were made *in situ* during the e-beam deposition.

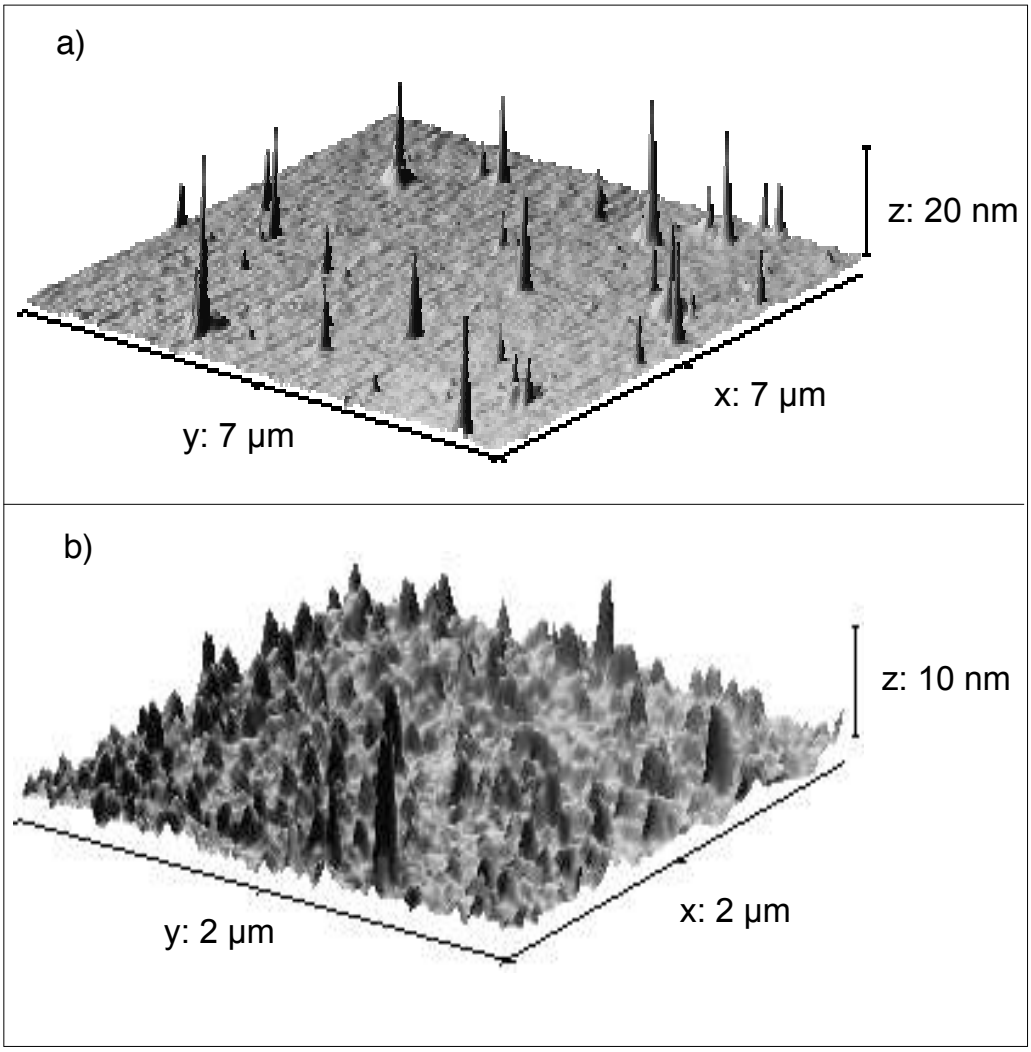

FIG. 2: The top panel is a high resolution AFM micrograph of a 5 nm thick CNi_3 film deposited onto glass at 84 K. The lower panel is a similar micrograph of 60 nm thick CNi_3 film. The spike-like structures are multi-wall carbon nantotubes.

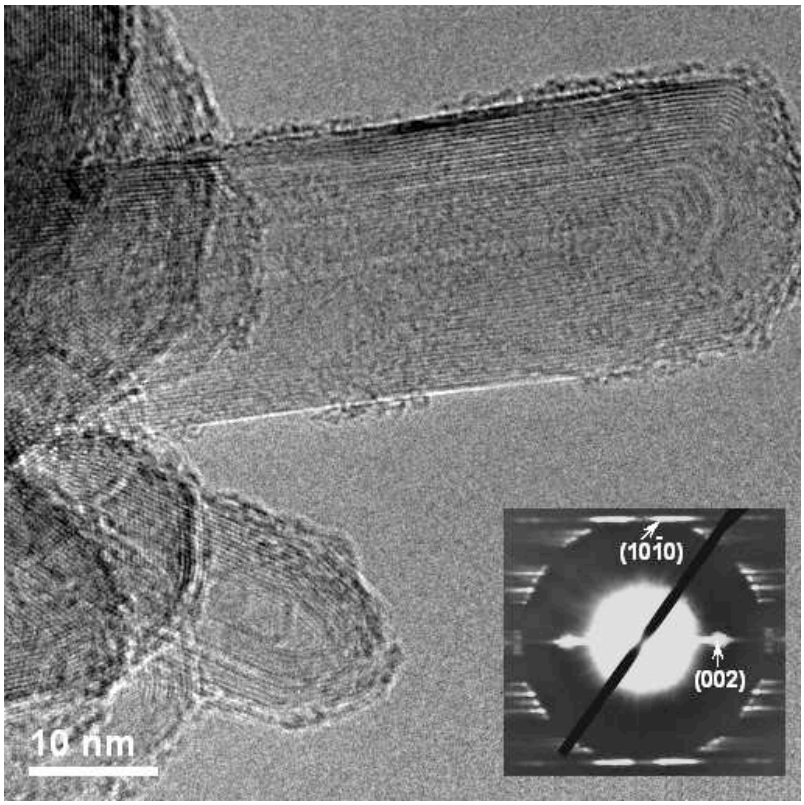

FIG. 3: TEM mircrograph of scrapings taken from a CNi_3 film deposited on a glass substrate at 84 K. Note that the structure consists of multiple walls encasing a hollow core. The inset depicts an electron diffraction pattern which is consistent with that of a multi-walled carbon nanotube.

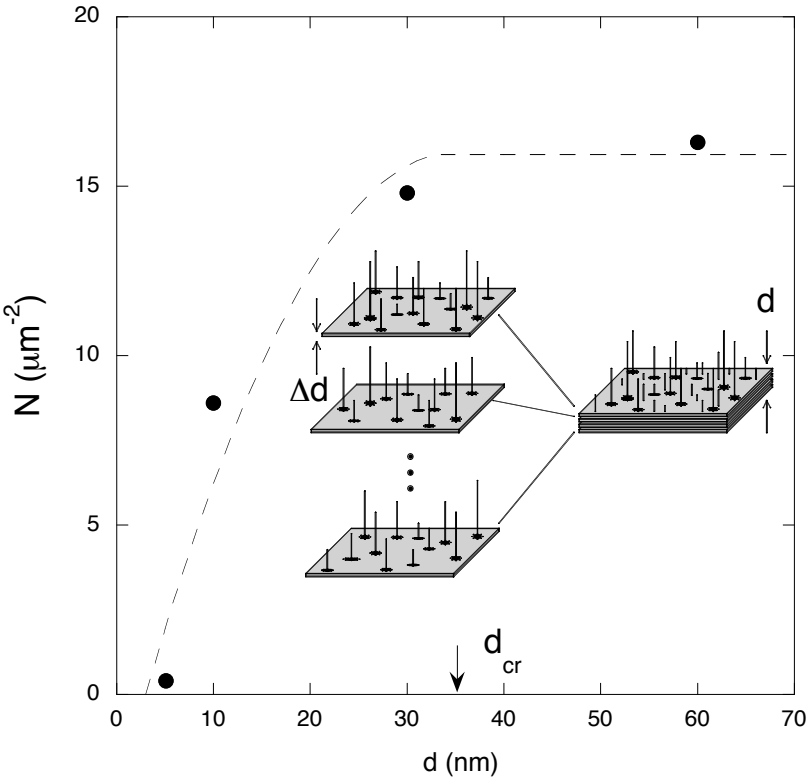

FIG. 4: Areal density of multi-wall carbon nanotubes as a function of CNi_3 film thickness. The dashed line represents a best fit of Eq. (1) to the data in which N_o and h_m were varied. Note that the density approaches zero at $d \approx 3$ nm. Inset: Our nanotube growth model assumes that a film of thickness d can be represented by a stack of minimally thick films each with an intrinsic nanotube population.

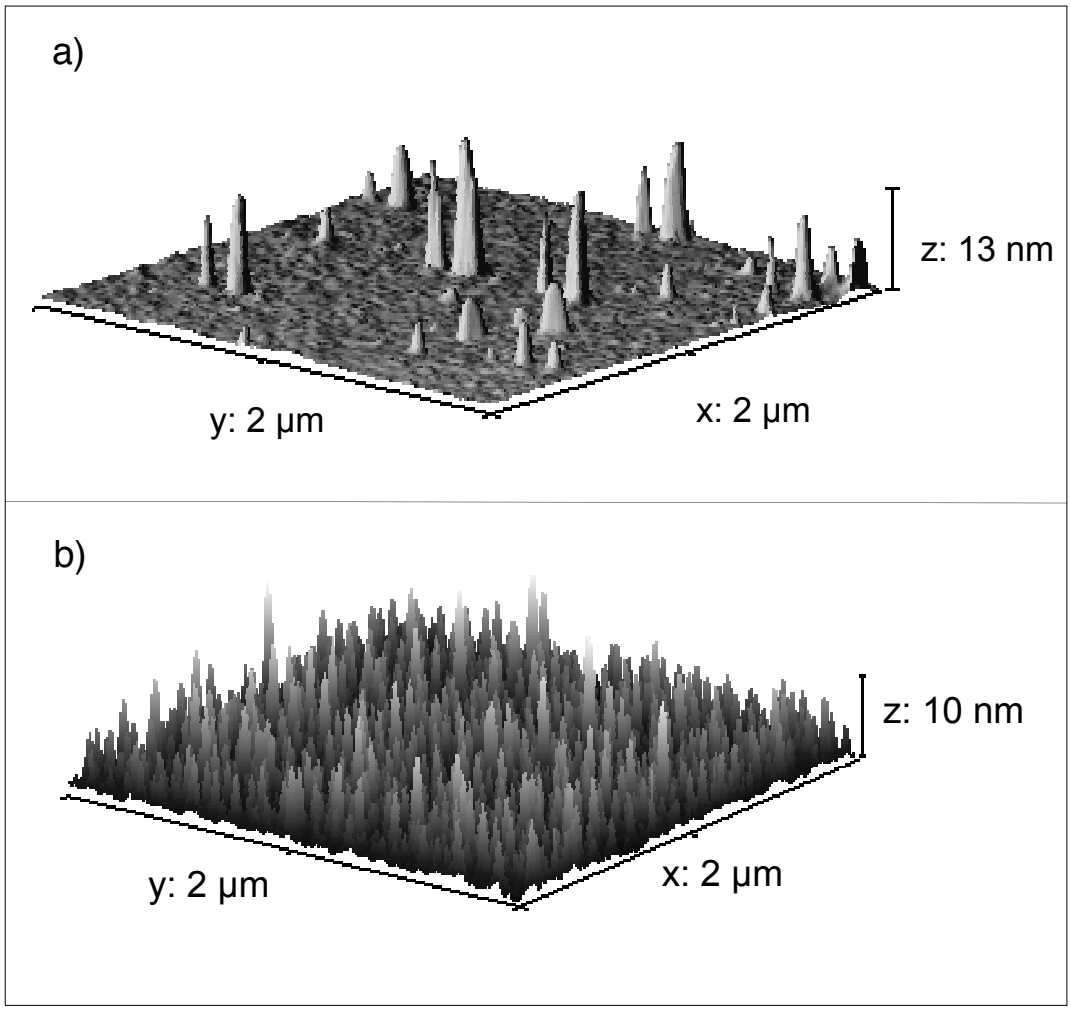

FIG. 5: AFM images of nanotube formation on a) fire-polished glass and b) crystalline sapphire. Both images were taken from 10 nm thick CNi_3 films deposited at 84 K.